RC22284 (W0112-050) December 18, 2001
Electrical Engineering

IBM Research Report

A comparative study of two transient analysis algorithms for lossy transmission lines with frequency-dependent data

Ibrahim Elfadel, A. E. Ruehli
IBM Research Division
Thomas J. Watson Research Center
P.O. Box 218
Yorktown Heights, NY 10598

H-M Huang
IBM Microelectronics Division
Route 52, Hopewell Junction, N.Y.
12533

A. Dounavis, M.S. Nakhla
Department of Electronics,
Carleton University, Ottawa ON,
K1S 5B6, Canada

Research Division
Almaden - Austin - Beijing - Delhi - Haifa - India - T. J. Watson - Tokyo - Zurich

A Comparative Study of Two Transient Analysis Algorithms for Lossy Transmission Lines with Frequency-Dependent Data

I. M. Elfadel* **H-M. Huang†** **A. E. Ruehli***

A. Dounavis♭ **M. S. Nakhla♭**

* **IBM T. J. Watson Research Center, P.O. Box 218, Yorktown Heights, NY 10598**

Tel: (914) 945-2278, Fax: (914) 945-4469, E-mail: {elfadel,ruehli}@us.ibm.com

† **IBM Microelectronics Division, Route 52, Hopewell Junction, NY 12533**

Tel: (845) 892-2723, Fax: (845) 892-2066, E-mail: haohuang@us.ibm.com

♭ **Department of Electronics, Carleton University, Ottawa, ON, K1S 5B6, Canada**

Tel: (613) 520-5780, Fax: (613) 520-5708, E-mail: {anestis, msn}@doe.carleton.ca

Abstract

Two general algorithms for the modeling of lossy transmission lines with frequency-dependent parameters are contrasted and compared. The first is based on the generalized method of characteristics while the second is based on a more recent Padé macromodeling approach. The different approximations made in these two algorithms are contrasted and computational evidence is presented to show that these two methods complement each other in their properties.

1 Introduction

The triple effect of increase in clock frequency, decrease in signal switching time, and increase in conductor packing density both at the chip and system level has pushed the issue of non-ideal

transmission line (TL) modeling and simulation to the forefront of both industrial and academic CAD research. Indeed, it is the case now that both the skin effect losses in the conductors and the shunt losses in the dielectrics contribute significantly to the degradation of the waveform [1]. The accurate handling of these effects has been made even more difficult by the fact that they need to be accounted for not just at the high frequencies of system operations, but also by the accompanying requirement that their measurement, modeling, and simulation be accurate over an ever widening frequency band, stretching from zero frequency for acceptable signal stability to many times the clock frequency for accurate prediction of timing and noise.

In this paper we consider two fundamentally different approaches to the macromodeling of lossy, dispersive, transmission lines (TL). The first approach belongs to the class of the generalized method of characteristics (MoC) [2] where the main idea is to represent the TL with a set of admittances and *delayed* sources representing the terminal behavior. The second approach is one of several that can be grouped together under the generic idea of *sectioning.* In this second class, delays are modeled implicitly and not extracted separately as in the method of characteristics.

The aim of this paper is to contrast and compare, conceptually and computationally, the two representative algorithms of these two classes, namely, the one based on [2, 3] for the method of characteristics and the one based on [4, 5] for a version of the sectioning method.[1]

The basic result of this study is that each of these two classes, which have not been compared before, has its own strengths and weaknesses. Basically, the first class seems to be best suited for the delay extraction of longer lines while the second class seems to provide acceptably fast

[1] Although there is no explicit segmentation of the line into small segments that can be modeled as RLGC circuits, this method exhibits similar behavior as explained in this paper.

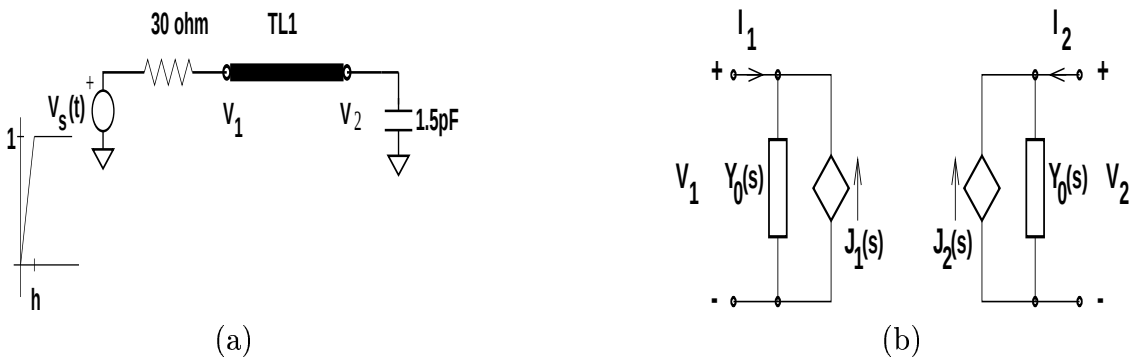

Figure 1: Transmission line circuit with driver and load (a) and MoC admittance equivalent model for the transmission line (b).

and accurate macromodels for shorter lines.

This paper is organized as follows. In Section 2, the fundamental aspects of the generalized method of characteristics (GMoC) are reviewed, especially the aspect related to the decomposition of the lossy TL into a lossless TL and a lumped attenuation circuit. The matrix Padé approximation method, which we take as a representative of the sectioning class, is reviewed in Section 3. We state a general formula to help clarify the tradeoffs that this method must overcome to produce acceptable TL macromodels. In Section 4, we give a detailed conceptual and algorithmic comparison between the two methods. The comparison encompasses some of the circuit-representation and implementation issues that might affect their ultimate efficiencies when integrated with SPICE-like circuit solvers. Rather than giving too many numerical examples, Section 5 treats just two examples: a single line case and a coupled case. The single-line case is dealt with in some depth to illustrate the various issues raised in this paper.

2 The Generalized Method of Characteristics

The starting point of the two methods mentioned above is the same, namely, the Telegrapher's first-order differential equations for the current and voltage written in the s domain as

$$\frac{dI}{dx} = -Y(s)V(x,s), \qquad \frac{dV}{dx} = -Z(s)I(x,s) \tag{2.1}$$

where

$$Y(s) = G(s) + sC(s) \quad \text{and} \quad Z(s) = R(s) + sL(s) \tag{2.2}$$

are, respectively, the parallel admittance and the series impedance of the transmission lines with $G(s), C(s), R(s), L(s)$ being the usual frequency-dependent per-unit-length (FDPUL) parameters. They are square matrices of order $n \times n$ for a transmission line system with $n+1$ conductors (n transmission lines and one reference conductor).

In one version of the method of characteristics, the wave propagation equation of the currents, namely,

$$\frac{d^2I}{dx^2} = Y(s)Z(s)I(x,s) \tag{2.3}$$

is solved with the boundary conditions $I(0,s) = I_1(s), V(0,s) = V_1(s)$ and $I(d,s) = -I_2(s), V(d,s) = V_2(s)$, where d is the length of the line. The pairs $(I_1(s), V_1(s))$ and $(I_2(s), V_2(s))$ are the current-voltage pairs at the input (near end) and output (far end) ports, respectively. In terms of these port vectors, the solution is expressed as

$$I_1(s) = Y_0(s)V_1(s) + J_1(s), \qquad I_2(s) = Y_0(s)V_2(s) + J_2(s) \tag{2.4}$$

where $J_1(s), J_2(s)$ are currents of controlled current sources whose values are given by

$$J_1(s) = -e^{-d\Gamma(s)}[Y_0(s)V_2(s) + I_2(s)], \qquad J_2(s) = -e^{-d\Gamma(s)}[Y_0(s)V_1(s) + I_1(s)] \tag{2.5}$$

with

$$\Gamma(s) = [Y(s)Z(s)]^{1/2} \quad \text{and} \quad Y_0(s) = \Gamma^{-1}(s)Y(s) \tag{2.6}$$

being the attenuation matrix and the characteristic admittance matrix, respectively. The equivalent circuit representing the current wave solution is shown in Figure 1(a). This equivalent circuit is at the basis of all device-level implementations of MoC in SPICE-like simulators. Among the earliest of such implementations for the multiconductor, lossy, frequency-dependent case was the one supported in IBM's ASTAP circuit solver [2], which is an earlier version of today's PowerSpice.

The MoC implementation presents many challenges in the coupled case. First, we should decouple the interactions between the conductors using a *characteristic* (or eigen) mode analysis of the attenuation matrix $\Gamma(s) = B(s)\Lambda(s)B(s)^{-1}$, where $\Lambda(s)$ is the diagonal matrix of the frequency-dependent eigenvalues (or characteristic values) and $B(s)$ is the frequency-dependent matrix whose columns are the eigenvetors of $\Gamma(s)$. The second implementation challenge is to find a consistent method for representing the frequency-dependent eigenvalues as well as all the frequency-dependent components of the eigenvector matrix $B(s)$ and the characteristic admittance matrix $Y_0(s)$.

Note that in terms of the eigendecomposition of the attenuation matrix $\Gamma(s)$, the propagation

matrix $P(s) = e^{-d\Gamma(s)}$ and the the characteristic admittance $Y_0(s) = \Gamma(s)^{-1}Y(s)$ can be expressed, respectively, as

$$P(s) = B(s)e^{-d\Lambda(s)}B(s)^{-1} \tag{2.7}$$

$$Y_0(s) = B(s)(\Lambda(s))^{-1}B(s)^{-1}Y(s). \tag{2.8}$$

The propagation and characteristic admittance matrices are known from measurements over a set of frequency points $\{\omega_k, 0 \leq k \leq N\}$ sampled from the frequency range $[\omega_{min}, \omega_{max}]$ of interest. At each of these frequencies the l-th eigenvalue $\lambda_l(j\omega_k)$ can be decomposed as

$$\lambda_l(j\omega_k) = \alpha_l(j\omega_k) + j\omega_k\tau_l(j\omega_k)$$

where the real part gives rise to a modal attenuation matrix

$$A(s) = e^{-d\alpha(s)}$$

while the imaginary part gives rise to a modal delay matrix

$$\Psi(s) = e^{-ds\tau(s)}.$$

When fitting complex functions to the entries of the different matrices occurring in Equations (2.7, 2.8, 2.4, 2.5) two types of functions must be handled. The first is a rational function

expressed in terms of poles and residues as

$$F(s) = \sum_{i=1}^{m} \frac{r_i}{s - p_i} \tag{2.9}$$

and the second is an irrational function that takes into account the frequency-dependent delays $\tau(s)$. Such a function can be expressed as

$$H(s) = r_0 e^{-d\tau_0 s} + \sum_{i=1}^{m} \frac{r_i e^{-ds\tau_i}}{s - p_i}. \tag{2.10}$$

The extraction of pure delays is the one fundamental difference between MoC and other methods belonging to the sectioning categaory.

There are several good algorithms for computing the poles and residues in the expressions of $F(s)$ and $H(s)$ based on measured data [6] or the paper by Chang, in [7]. In our own implementation of the method of characteristics, we used the vector fitting approach in [8]. The main reason for modeling the matrix entries as in (2.9) or (2.10) is to be able to map the Laplace domain solutions back to the time domain. While the lossless case is easy to handle (simple delay of the time-domain waveform), the lossy case leads to time-domain convolutions that can be computationally costly. One way around this problem is to use recursive convolutions [9], which is the method adopted in this paper. Another possiblity beside recursive convolutions is to use the expressions of $F(s)$ and $H(s)$ to come up with equivalent circuits containing ideal transmission lines (to represent pure delays), resistors, capacitors, and controlled sources. These equivalent circuits can be directly incoporated in the circuit solver and simulated using its integration engine. Such an approach is described in [10].

3 The Method of Rational Matrix Approximations

3.1 The Method of Matrix Padé Approximations

Instead of solving the wave propagation equation (2.4) to get the port currents in the s-domain, the Matrix Padé Approximation (MPA) method [4, 5] solves the first-order linear system (2.1) using the matrix exponential function to get the hybrid $2n$-port representation

$$\begin{bmatrix} V_2(s) \\ -I_2(s) \end{bmatrix} = e^{-d[\Phi(s)]} \begin{bmatrix} V_1(s) \\ I_1(s) \end{bmatrix} \quad \text{with} \quad \Phi(s) = \begin{bmatrix} 0 & Z(s) \\ Y(s) & 0 \end{bmatrix} \tag{3.11}$$

Denoting by $T(s) \equiv e^{-d[\Phi(s)]}$ the transfer matrix from the near end (ports 1) to the far end (ports 2), MPA approximates this matrix using the matrix rational fraction of order (N, N)

$$T(s) \approx [P_{N,N}(d\Phi(s))]^{-1} Q_{N,N}(d\Phi(s)) \tag{3.12}$$

$$P_{N,N}(d\Phi(s)) = \sum_{k=0}^{N} c_{N,k} [d\Phi(s)]^k \tag{3.13}$$

$$Q_{N,N}(d\Phi(s)) = P_{N,N}(-d\Phi(s)) \tag{3.14}$$

$$c_{N,k} = \frac{(2N-k)!N!}{(2N)!k!(N-k)!} \tag{3.15}$$

Note that the coefficients $c_{N,k}$ are known *a priori*. However the coefficients of the polynomial matrices $P_{N,N}(d\Phi(s))$ and $Q_{N,N}(d\Phi(s))$ in s are problem-dependent and must be computed using the $R(s), L(s), G(s), C(s)$ data. There are a number of alternatives for exploiting the above approximation to model the transmission lines in the time-domain [4, 5]. These alternatives are

all based on the fact that this frequency-domain matrix rational fraction can be translated into the time domain using either state-space matrices or RCL circuits.

It is important to note that the validity of the above approximation depends on the size of the quantity $d\ \Phi(s)$. For a given order N, the closer this quantity is to zero the better the approximation of the exponential matrix. In particular, for a given PULFD parameters, the smaller d, i.e., the shorter the line, the better the approximation. For long lines, the approximation accuracy will degrade rapidly, and line segmentation will be needed based on the observation

$$T(s) = \left(e^{\left[-\frac{d}{m}\Phi(s)\right]}\right)^m \approx \left(\left[P_{N,N}\left(\frac{d}{m}\Phi(s)\right)\right]^{-1} Q_{N,N}\left(\frac{d}{m}\Phi(s)\right)\right)^m . \tag{3.16}$$

The tradeoffs between the length d, the number of segments m, and the order N for a given set of PULFD parameters have to be determined automatically to insure the robustness and accuracy of this method.

Another remark is that there is some affinity between the MPA method and transmission-line macromodeling techniques based on moment matching [11, 12]. In the latter, $T(s)$ is expanded in a Taylor series in the neighborhood of $s = 0$, and the matrix coefficients of the powers of s are determined recursively. This is to be contrasted with MPA where $T(s)$ is expanded in a Padé rational fraction in the neighborhood of $d = 0$.

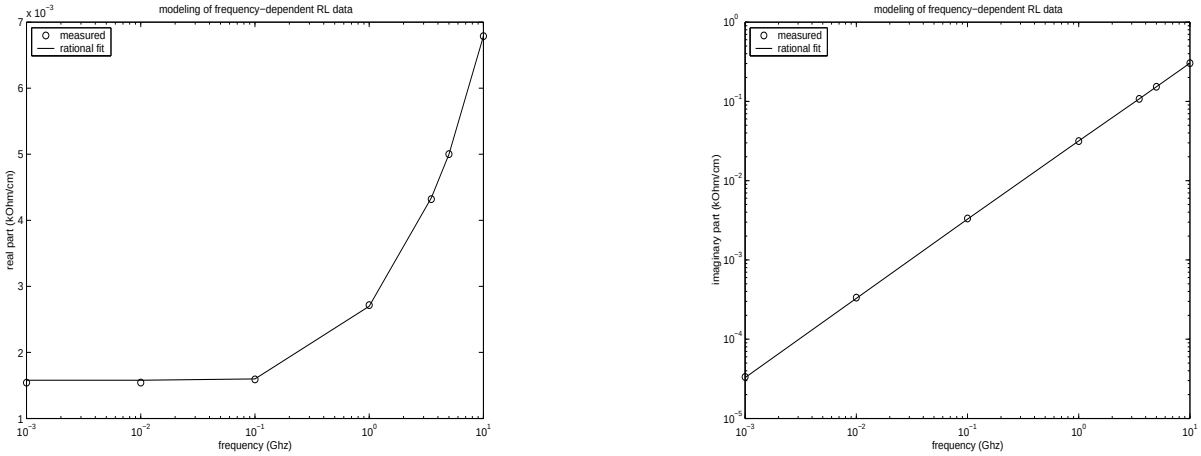

Figure 2: Fitting of the FDPUL with a 3-section RL ladder: (a) resistance (b) reactance.

3.2 The Modified Matrix Padé Approximation

An important advantage of the MoC approach is that, since it extracts the line delay explicitly, the corresponding transient responses generally do not exhibit spurious ripples in the early-time region. Most passive macromodeling schemes [13, 14, 15], including the MPA algorithm described in the previous sections, employ some kind of approximation in the frequency-domain to match the impulse response up to a maximum frequency of interest f_{max}. However, the behavior above f_{max} is generally not considered, which can lead to errors in the impulse transient response (especially in the early-time period). This can affect the accuracy of the transient response at all other time points when the macromodel is included during the simulation of a large circuit. Also, the above problem can be aggravated in the presence of sharp rise times or with smaller capacitive loads. To remove these ripples, the order of the approximation required would be very high, making the macromodel inefficient. In order to address the above problem, the MPA algorithm has been modified [16]. The new method provides a mechanism to control the

asymptotic behavior of the high-frequency impulse response while matching the response up to f_{max} accurately. This leads to significant reduction in errors of transient responses. Also, it guarantees the passivity of the macromodel.

The main concept of the modified MPA algorithm can be explained as follows. The early-time impulse response is mainly influenced by the following relationship:

$$h(0^+) = \lim_{s \to \infty} sH_{MN}(s) \tag{3.17}$$

where s is the Laplace operator, and $H_{MN}(s)$ represents the frequency-domain rational function, M and N are the numerator and denominator polynomial orders, respectively, and $h(0^+)$ represents the early-time response ($t = 0$). Assuming that the all the dereivatives of the impulse response up to order k are zero, $h^{(l)}(0^+) = 0, 0 \leq l \leq k$, then

$$h^{(k+1)}(0^+) = \lim_{s \to \infty} s^{k+1} H_{MN}(s) \tag{3.18}$$

Observing Equations (3.17) and (3.18) one can note that, to obtain flat response around $t = 0$, the transfer admittances represented by $H_{MN}(s)$ must be a strictly proper rational functions such that $k = N - M$ is maximum, while preserving the accuracy of the macromodel. Also, it is desired that the order of the denominator (N) is kept as minimum as possible for achieving efficient simulation. The above principles are used to reduce the error in transient responses of the MPA algorithm. Details of the algorithm can be found in [16].

f(GHz)	0.0	10^{-3}	10^{-2}	10^{-1}	1.0	3.5	5.0	10.0
R(Ω/cm)	1.54	1.54	1.54	1.59	2.72	4.32	5.00	6.79
L(nH/cm)	5.43	5.31	5.32	5.31	5.03	4.90	4.87	4.83

Table 1: Frequency-dependent data of the single line in Figure 1(b)

4 Contrasting the Two Methods

The fundamental idea behind all the transient-analysis algorithms for lossy transmission lines is to find approximate inverse Laplace transforms for the transcendental matrix functions encountered in the exact s domain solutions. See Equations (2.4, 2.5, 3.11). In both the method of characteristics and the matrix Padé approximation, the transcendental function is an exponential. But while the propagation matrix $P(s) \equiv e^{-d\Gamma(s)}$ has an $n \times n$ matrix in the argument of its exponential, the transfer matrix $T(s) \equiv e^{-d\Phi(s)}$ has a $2n \times 2n$ matrix argument. The relationship between $\Phi(s)$ and $\Gamma(s)$ is given by

$$\Phi^2(s) = \begin{bmatrix} \Gamma^2(s) & 0 \\ 0 & (\Gamma^T(s))^2 \end{bmatrix} \tag{4.19}$$

Hence, the matrix $\Phi(s)$ is *one* of the square roots of the block diagonal matrix $diag(Z(s)Y(s), Y(s)Z(s))$. Another square root is of course $diag(\Gamma(s), \Gamma(s)^T)$. Next, we contrast the way $P(s)$ is handled in MoC with the way $T(s)$ is handled in MPA.

1. *Transmission line circuit representation:* As mentioned previously, MoC uses either an admittance or an impedance representation for the $2n$-port transmission line while MPA use a hybrid representation. In this paper, we use the admittance representation for MoC

because it is the one providing the MNA-compatible stamp.

2. *Computation of the exponential function:* In MoC, this is done by diagonalizing the matrix $Y(s)Z(s) = B(s)\Lambda^2(s)B^{-1}(s)$, computing its square root $\Gamma(s) = B(s)\Lambda(s)B^{-1}(s)$, and concluding that $P(s) = B(s)e^{-d\Lambda(s)}B^{-1}(s)$. Note that this value of $P(s)$ is exact. On the other hand, in MPA, no eigen analysis is used, and the matrix $T(s)$ is approximated with the matrix rational fraction according to (3.12). One intriguing possibility for obtaining TL macromodels is to apply MPA, not to the exponential matrix $T(s)$, but to the exponential matrix $P(s)$.

3. *Rational function approximation:* Even when the data for a lossy TL is *independent* of frequency, MoC must fit rational functions to the components of the eigenvalue and eigenvector matrices $\Lambda(s), B(s)$. Tracking the eigenmodes along the frequency axis is also needed as they may not occur in the same order when the frequency point is changed. In MPA, rational function fitting is needed only when the lossy data is dependent on frequency. Note that for the case of coupled symmetric lines with equal losses, the MoC modal analysis is trivial *even* in the frequency-dependent case as it can be reduced to the study of common and differential propagation modes.

4. *Pure delay extraction:* One very important feature of MoC is that the rational functions used to model the eigenvalue matrix $e^{-d\Lambda(s)}$, incorporate the approximation $e^{-d\lambda_k(s)} \approx e^{-d\tau_k s}A_k(s)$, where τ_k represents the pure delay of the k-th mode and $A_k(s)$ is its attenuation function. This extraction of the pure modal delays amounts to decomposing the transient analysis of the lossy transmission line into a lossless line in which the signals are delayed but not attenuated and a lumped circuit to account for the signal attenuation. No such

delay extraction or lossy/lossless decomposition is used in MPA. Note that the pure delay extraction in MoC allows the attenuation functions to be approximated with low order rational function. In MPA, the accurate accounting for the line delay, especially in long lines, will require high Padé-approximation orders or a large number of line segments.

5. *Fitting of frequency-dependent data:* In MoC, the dependence of the PUL parameters, $R(s), L(s), G(s), C(s)$ on frequency is accounted for indirectly, i.e, by fitting transfer matrices not to the immittances $Y(s)$ and $Z(s)$ but to the propagation matrix $P(s)$ and the characteristic admittance $Y_0(s)$. In MPA, the fitting of the FDPUL, is done directly on the $Y(s)$ and $Z(s)$. This latter fitting has the advantage that good fit can be achieved with real, stable poles and zeros while the MoC fitting might require complex poles and zeros. Moreover in MoC, unstable poles might be generated unless additional (nonlinear) constraints are imposed on the fitting procedure [17].

6. *Passivity:* According to [4, 5], the Padé macromodel generated using (3.12) is passive. Moreover, the frequency-dependent losses can be modeled using passive driving-point matrices and the latter inserted in the Padé rational matrix to yield an overall TL model that is also passive. Modulo the extracted modal delays, MoC has no guarantee of passivity for the rational matrices it produces for fitting the eigenvector matrix $B(s)$ or the modal attenuation functions $A_k(s)$. It is possible that removing the passivity constraint might result in a lower error for the estimated parameters and therefore better models.

7. *Equivalent-circuit representation:* The MoC TL model of Figure 1(a) is a strict circuit-model [18] in the sense that it has the same number of nodes as the line it represents. In MPA, equivalent-circuit representations having R, L, G and C lumped elements as well as

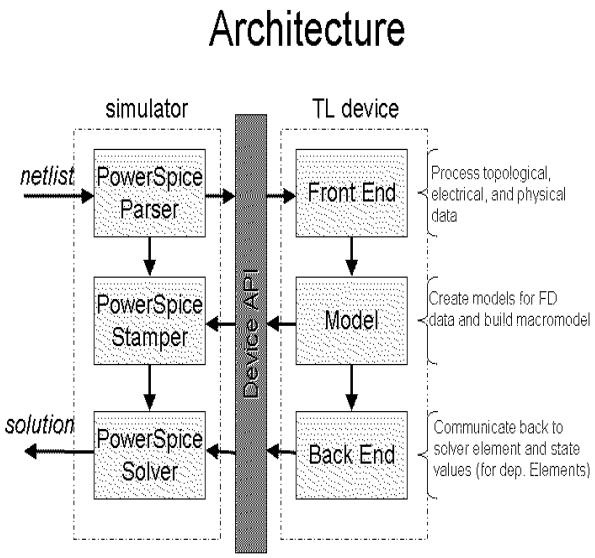

Figure 3: Communication architecture between the transmission line macromodel and the circuit solver (IBM's PowerSpice). The communication is managed by the Application Programming Interface (API).

ideal transformers can be synthesized and incorporated in the circuit netlist. These latter representations result in an increase of the the numbers of nodes and circuit elements. Numerical evidence [5] suggests that these equivalent circuits are more efficient that those based on finite-difference approximations of (2.1), which is the case for the U-element model in HSPICE.

8. *Macromodel Representation:* For both MoC and MPA, there are many possibilities for the macromodel representation, including rational fraction, state-space, MNA stamp, and pole-residue representations. The specific choice depends on the time-domain integration algorithm. For recursive convolution, the pole-residue representation is the most appropriate. The vector fitting method of [8] is used in our implemenation of the MoC algorithm. This method computes the pole-residue representation directly. The typical least-square

fitting algorithm results in a rational fraction, which has to be transformed into a pole-residue form if it is be used in a recursive convolution algorithm.

9. *Time-domain solution:* When implemented as a circuit netlist, the MPA or MoC macromodel will use the circuit solver integration engine and no special algorithm is needed for obtaining the time-domain waveforms. On the other hand, when no equivalent-circuit is used, a special integration engine must be part of the macromodel. The two classical solution methods have been recursive convolution [3] and state-space integration [2, 17].

10. *Integration with SPICE-like simulators:* As noted in [18], TL macromodels can be integrated with the SPICE-like circuit solver either as a device (i.e., no nodes added to the netlist) or as an equivalent circuit. Note that when the simulator supports a circuit API software layer [19], the MPA equivalent circuit can be generated on-the-fly in a module of its own that would connect to the rest of the netlist through the $2n$ ports of the transmission line.

Our implementations of both algorithms are structurally the same, and the common architecture of both implementations is given in Figure 3. The transmission line macromodel is a dynamically loadable library (DLL) that communicates with the circuit solver (in our case IBM's PowerSpice) using the application programming interface (API) described in [19]. This interface extends the circuit solver functionality by allowing the user to code portable, compact circuit models without compromising the integrity of the circuit solver. The API implementations of MoC and MPA described in this paper differ in the *contents* of the front-end, model, and back-end modules, Figure 3. For instance, while the **model** module for MoC is represented, for a single line, by a

circuit similar to that of Figure 1(b), the MPA **model** for the same line, contains an RLC circuit whose template is given in [4]. The size of the circuit depends on the MPA macromodel order, the line length, and the orders of the models representing the frequency-dependent data.

5 Numerical Examples

5.1 Single Line

In order to illustrate some of the points raised in the previous section, we use the single transmission line of Figure 1(b) with the FDPUL parameters shown in Table 4. For this line we have $C(s) = 2.24pF/cm$, and $G(s) = 0.0$. The frequency-dependent data are modeled using a 3-section RL ladder. The goodness of the resulting fitted circuit model is illustrated in Figure 2 which shows an excellent match for the imaginary part of the data (i.e, the reactance ωL) and a very good agreement for the real part of the data, the resistance, especially, at high frequencies. This equivalent-circuit is used in a number of MPA macromodels of the transmission line that differ in the order N of the Padé approximation in (3.12). For each MPA order six instances of the transmission line ranging in length from $d = 2.5cm$ to $d = 10cm$ are modeled and compared with the simulation results using MoC. Figure 4 shows that for a line of length 2.5 cm, there is an excellent agreement between MoC and an MPA macromodel of order 8 for both the far end and the near end signals. For an MPA macromodel of lower order, residual high-frequency oscillations is observed. MPA does not require segmentation of the line into small segments as is the case for finite difference macromodeling [20]. However the observed high-frequency oscillations

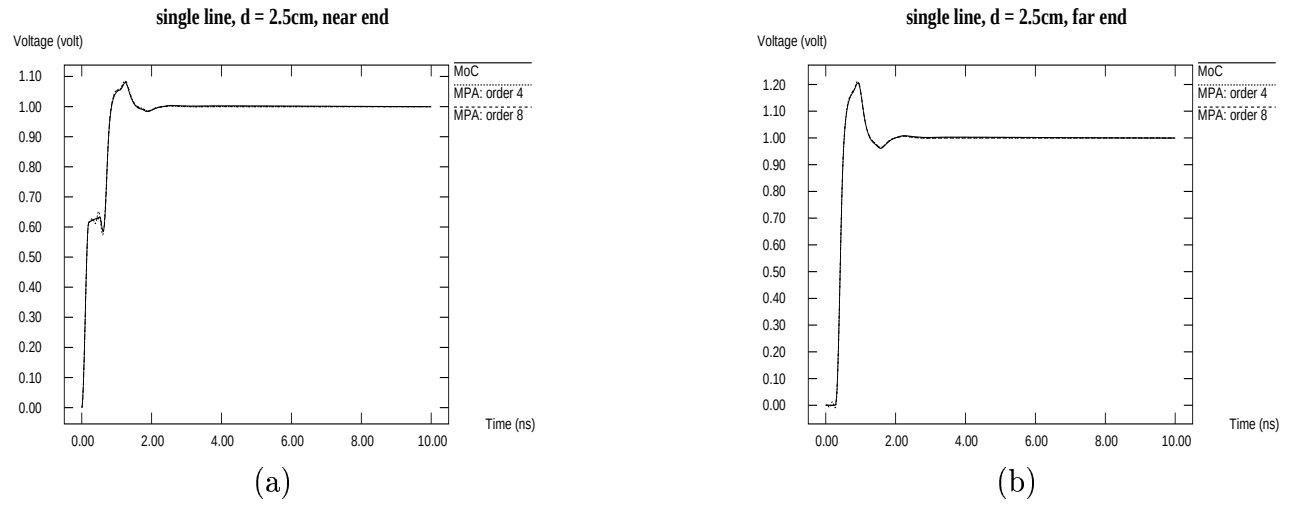

Figure 4: Comparison between MoC and MPA for the single line of Figure 1(a). Length = 2.5 cm: (a) near end (b) far end.

are of the same nature in that they result from approximating a distributed-parameter system with a finite-dimensional one. In MPA, one way of canceling these oscillations is to increase the Padé approximation order N. As in the case of lumped LC delay lines used to model lossless transmission lines, one should expect that the longer the line, the higher the Padé order needed to capture the initial line delay. Figure 5 shows good agreement between MoC and MPA for a line of length $d = 10cm$ for a higher-order model with $N = 20$. This need for higher order Padé can also be understood in light of the fact that MPA is based on a rational expansion of the transfer matrix $T(s)$ around the point $d = 0$, where d represents the line length. Hence, long lines will require more terms in the expansion to get an acceptable approximation.

The maximum absolute value of the difference between the MoC waveform and the MPA waveform over the simulation interval is given in Figure 6 for both the near end (a) and the far end (b). These two plots summarize quite well the behavior of MPA relative to MoC. They show that for a given line length the worst-case difference between MoC and MPA decreases

with the order of the MPA macromodel. This decrease exhibits a "knee" beyond which higher MPA orders have little effect on the accuracy of MPA relative to MoC. The difference between MoC and MPA is due to two factors. The first is the intrinsic difference that results from the fact that MPA and MoC have different algorithms for modeling the frequency-dependent data. The second factor is due to the spurious oscillations inherent to low-order macromodels of the sectioning type. Our experiments suggest that in the "steep slope" region (before the knee), Figure 6, it is the difference due to high-frequency oscillations that dominates while in the "flat" region (after the knee) it is the difference due to data modeling that dominates. One should note though that the amplitude of the MPA oscillations is affected by the amount of truncation error tolerated in the circuit solver. Moreover, there is numerical evidence that the approximation $T(s) \approx [P_{N+1,N+1}(d\Phi(s))]^{-1} Q_{N,N}(d\Phi(s))$ yields oscillatory amplitudes which are smaller than those of (3.12). Another point that these figures illustrate is that for a given MPA order N, the shorter the line the smaller the difference. This suggests that MPA needs to be combined with a line segmentation strategy that would aim at optimizing the tradeoffs between the order, the number of segments, and the line length. See (3.16).

Finally, whether the improvement in MPA accuracy relative to MoC is accomplished using a larger number of line segments of a lower Padé macromodel order, or one segment with a higher Padé macromodel order, one should look at all the costs that this improvement entails. This

Macromodel	MoC	4	8	12	16	20	24
d = 2.5cm	0.70	0.33	0.56	0.50	0.65	0.80	0.97
d = 10cm	0.69	0.33	0.52	0.48	0.66	0.82	1.06

Table 2: CPU times (sec) for MoC and MPA. The Padé orders of MPA are 4 through 24.

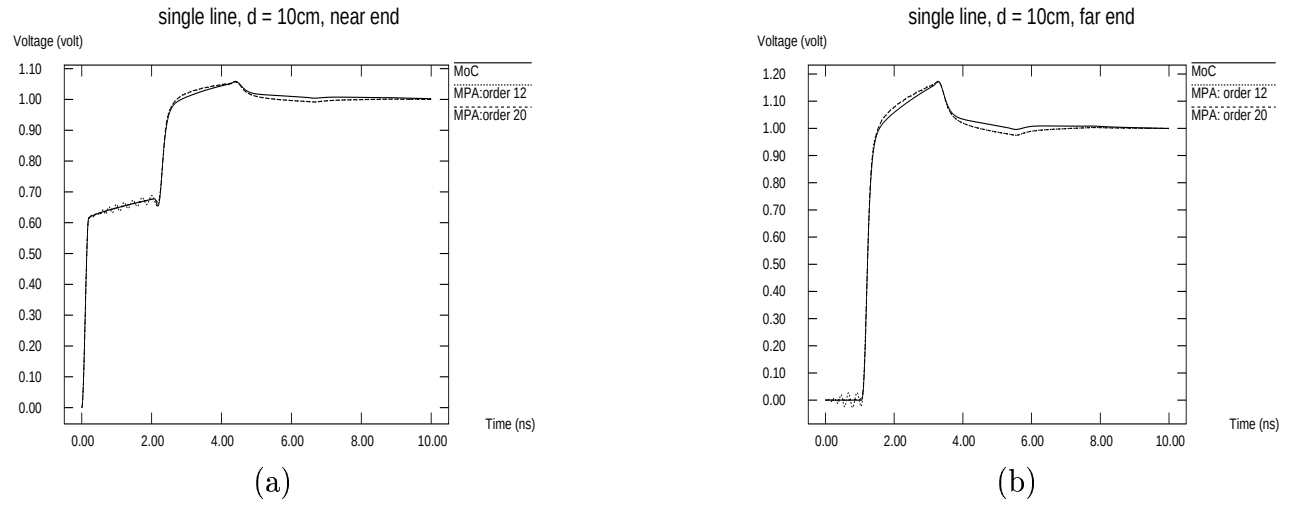

Figure 5: Comparison between MoC and MPA for the single line of Figure 1(a). Length = 10cm: (a) near end (b) far end.

is illustrated in Table 2 where the CPU times for simulating the MoC and MPA models are exhibited. This table suggests that for longer lines to overcome the MPA oscillations, the order needed might result in a macromodel that is "slower" than MoC. Note that such CPU comparisons are made possible only because both algorithms have been fully implemented as callable macromodels by the circuit solver.

5.2 Coupled Line

The second example deals with a lossy coupled line with both its resistive and dielectric losses dependent on frequency. The line length is $d = 10cm$. The FDPUL inductance and resistance are shown in Table 3. The FDPUL capacitance is given by $(C_{11}, C_{12}) = (1.371, 0.02455)$. For this coupled line, we have $R_{22} = R_{11}, L_{22} = L_{11}, C_{22} = C_{11}, R_{21} = R_{12}, L_{21} = L_{12}, C_{21} = C_{12}$. The dielectric loss tangent is $tan\delta = 0.0025$. The coupled line is driven and loaded as shown in

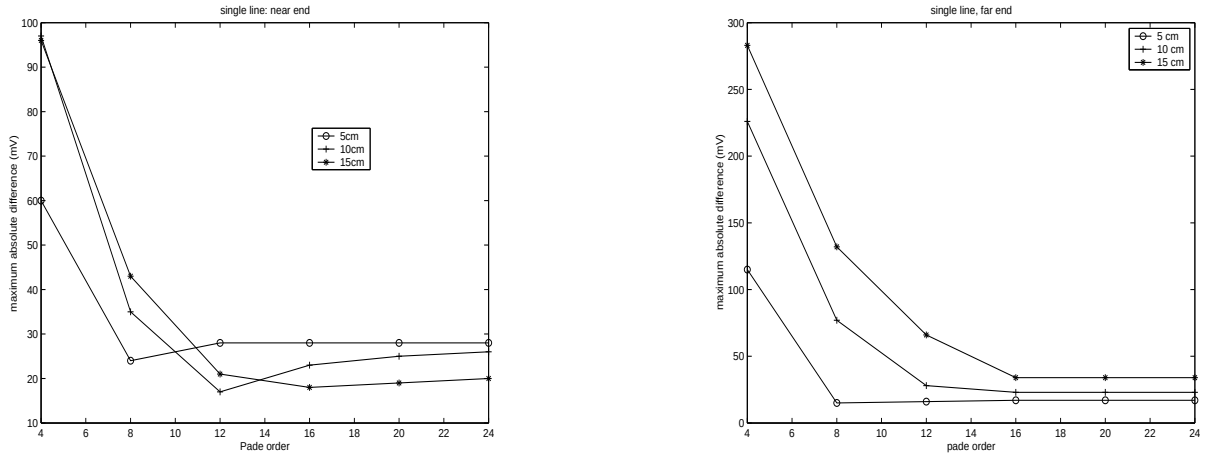

(a) (b)

Figure 6: Voltage difference plots for MoC and MPA for the single line of Figure 1(a): (a) near end (b) far end.

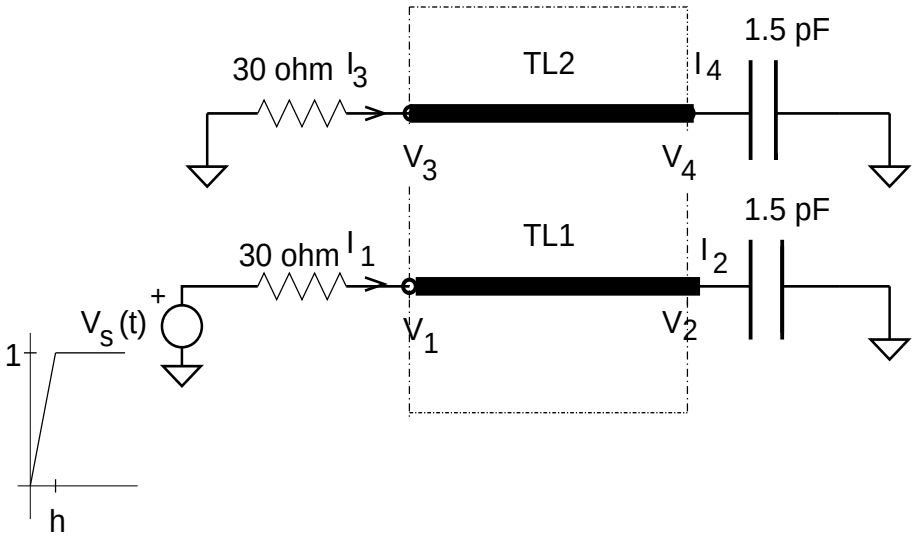

Figure 7: Coupled transmission line with its drivers and loads. Input ramp is 20ps.

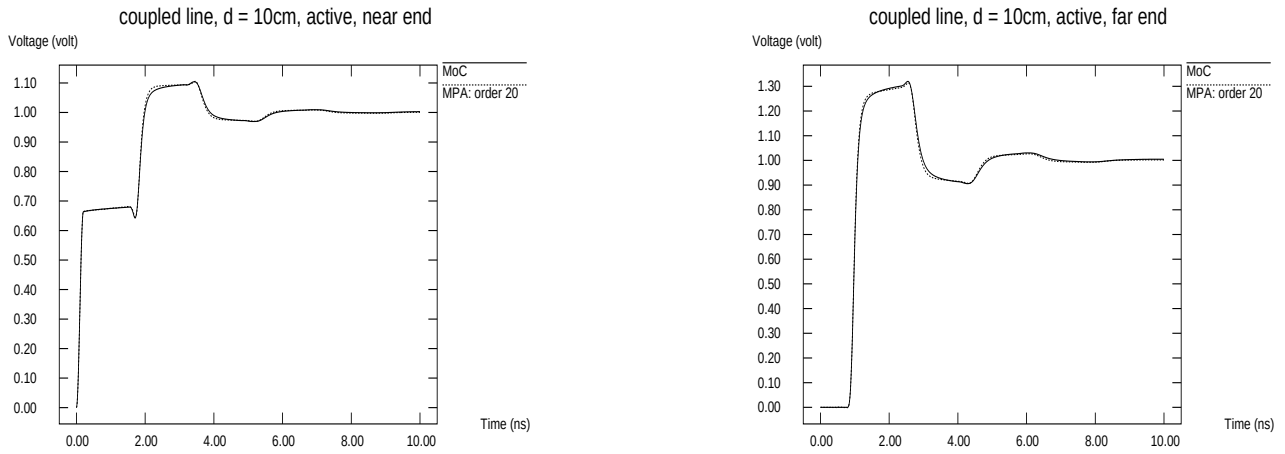

Figure 8: Comparison between MoC and MPA for the coupled line of 7. Active line: (a) near end (b) far end.

Figure 7. The input signal into the active line switches from 0 to 1 volt in 20ps.

The MPA macromodel used to model this coupled line has order 20. Figure 8 shows excellent agreement between MoC and MPA for the behavior of both the near and far end of the active line. We also have very good agreement for the quiet line, Figure 9, although the MPA quiet near end exhibits small spurious oscillations with respect to the MoC quiet near end.

This example illustrates the fact that both MoC and MPA can model frequency-dependent dielectric losses in a consistent manner. It also indicates that the correct modeling of coupling in

freq. (GHz)	0.0	0.0033	0.0066	0.01	0.033	0.066	0.1	0.3	0.66	1.0	3.5	6.6	10.0
L_{11} (nH/cm)	6.59	6.16	5.75	5.52	5.20	5.09	5.01	4.87	4.77	4.73	4.69	4.67	4.66
L_{12} (nH/cm)	0.43	0.33	0.23	0.26	0.26	0.26	0.26	0.26	0.26	0.26	0.25	0.25	0.25
R_{11} (Ω/cm)	0.29	0.33	0.34	0.35	0.39	0.45	0.51	0.53	0.82	1.03	2.46	5.36	7.49
R_{12} (Ω/cm)	0.0	0.029	0.03	0.03	0.03	0.03	0.031	0.04	0.06	0.08	0.2	0.4	0.55

Table 3: Per-unit-length inductance and resistance parameters of the coupled transmission line.

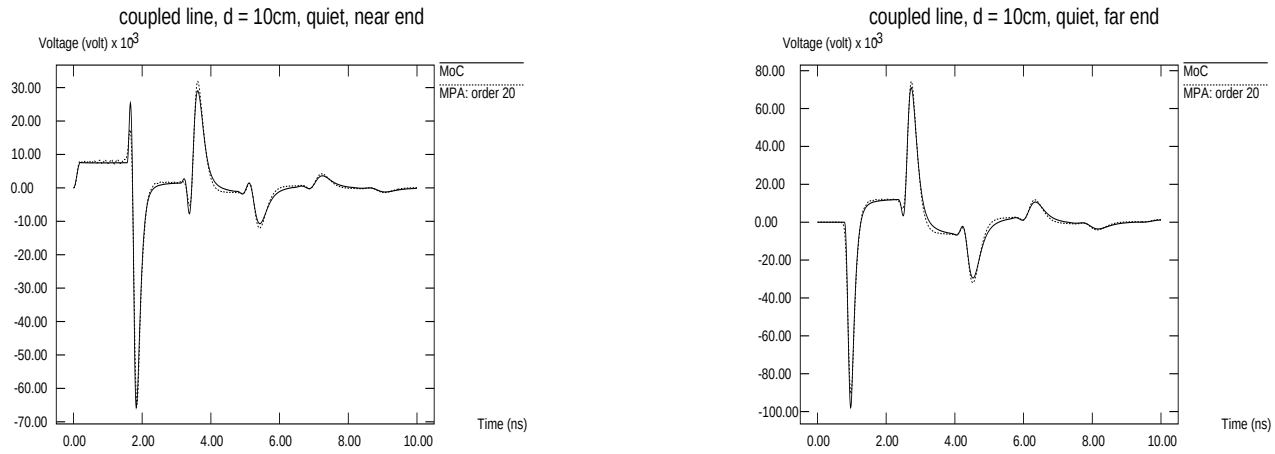

(a) (b)

Figure 9: Comparison between MoC and MPA for the coupled line of 7. Quiet line: (a) near end (b) far end.

the MPA case might require higher-order models than in the single-line case, especially when it is important to eliminate spurious oscialltions. It is worth noting that for this particular example, the MPA macromodel resulted in a CPU speedup with respect to MoC of about 1.5X

In order to illustrate the advantage of the modified MPA algorithm [16] in this particular example, Figure 10 compares, for the quiet line of Figure 7, the transient response of the circuit obtained using the MPA and the modified MPA algorithms. The plots clearly show the improvement in suppressing the spurious ripples in the early time response. The comparison shows that for this example, the accuracy obtained using the modified MPA with order $N = 9$ is equivalent to the accuracy of the MPA with order $N = 20$. In other words, for the same order N, the modified MPA yields better accuracy than the MPA algorithm. Equivalently, for the same accuracy, a lower order models can be obtained using the modified MPA. Especially for relatively long lines.

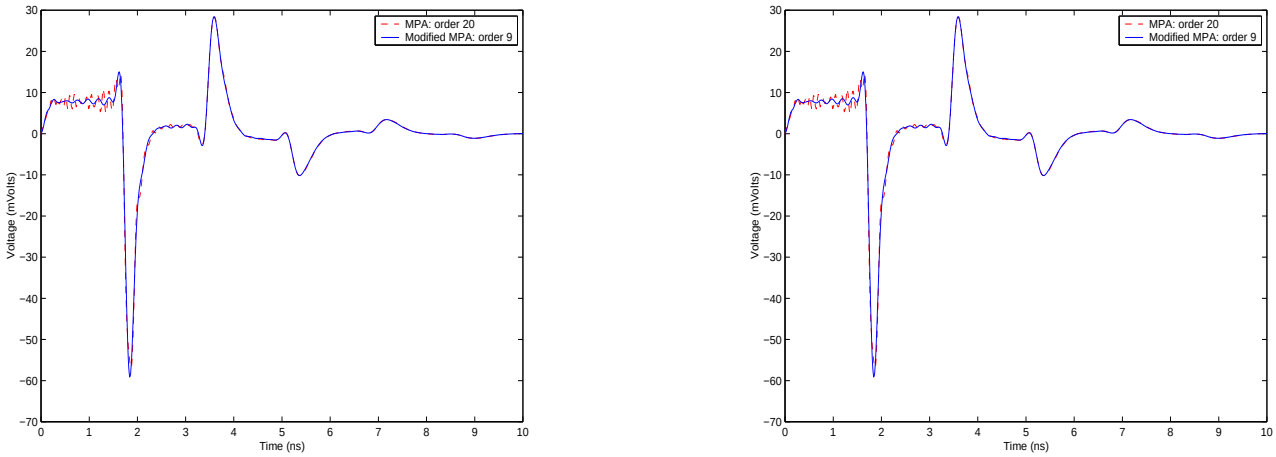

(a) (b)

Figure 10: Comparison between MPA and modified MPA for the coupled line of 7. Quiet line: (a) near end (b) far end.

6 Conclusions

This comparative study of two algorithms for transmission line modeling, namely, the generalized method of characteristics (MoC) and the matrix Padé approximation (MPA) suggest that each has its own strengths and weaknesses. MoC seems to perform very well when it comes to the extraction of delays for long lines while MPA provides acceptably accurate and fast macromodels for short lines. One practical example where MoC seems to be faster than MPA are long, relatively lossless, coaxial cables of a length of several meters. On the other hand MPA seems to be faster than MoC for the global interconnect used in on-chip wiring and shorter board wires. For the *large* domain in between, an automatic criterion for determining the more appropriate method would be highly desirable.

Acknowledgments

We would like to acknowledge the helpful discussions we have had with J. Garrett-Hoffman, R. Kimmel, D. Becker, Z. Chen, and G. Katopis from IBM. We also thank B. Agrawal, P. Coteus, and L. Stok from IBM for their managerial support. A. Deutsch provided us with a preprint of [1].

References

[1] A. Deutsch, G. V. Kopcsay, P. W. Coteus, C. W. Surovic, P. E. Dahlen, D. L. Heckmann, D. W. Duan. Frequency-dependent losses on high-performance interconnections. *IEEE Transactions on Advanced Packaging*, 43(4):446–565, November 2002.

[2] A. J. Gruodis and C. S. Chang. Coupled lossy transmission line characterization and simulation. *IBM Journal of Research and Development*, 25(1):25–41, January 1981.

[3] S. Lin and E. S. Kuh. Transient simulation of lossy interconnects based on recursive convolution formulation. *IEEE Transactions on Circuits and Systems, I*, 39(11), November 1992.

[4] A. Dounavis, X. Li, M. S. Nakhla, and R. Achar. Passive closed-form transmission-line model for general-purpose circuit simulators. *IEEE Transactions on Microwave Theory and Techniques*, 47(12):2450–2459, December 1999.

[5] A. Dounavis, R. Achar, and M. S. Nakhla. Efficient passive circuit models for distributed networks with frequency-dependent parameters. *IEEE Transactions on Advanced Packaging*, 22(3):382–392, August 2000.

[6] J. P. Marti. Accurate modelling of frequency dependent transmission lines in electromagetic transient simulation. *IEEE Transactions on Power Apparatus and Systems*, PAS-101:147–155, January 1982.

[7] A. E. Ruehli, Ed. *Circuit analysis, simulation and design, Part 2.* Elsevier Science Publishers B. V. (North-Holland), 1987.

[8] B. Gustavson and A. Semlyen. Rational approximation of frequency domain response by vector fitting. *IEEE Transactions on Power Delivery*, pages 1052–1061, July 1999.

[9] A. Semlyen and A. Dabuleanu. Fast and accurate switching transient calculations on transmission lines with ground using recursive convolution. *IEEE Transactions on Power Apparatus and Systems*, PAS-94:561–569, March 1975.

[10] S. Grivet-Talocia, I. A. Maio, and F. Canavero. Recent advances in reduced-order modeling of complex interconnects. In *Digest of Electr. Perf. Electronic Packaging*, volume 10, Cambridge, MA, October 2001.

[11] E. Chiprout and M. S. Nakhla. *Asymptotic waveform evaluation.* Kluwer, 1994.

[12] M. Celik and A. C. Cangellaris. Efficient transient simulation of lossy packaging interconnects using moment-matching techniques. *IEEE Transactions on Components, Packaging, and Manufacturing Technology-Part B*, 19(1):64–73, February 1996.

[13] A. Odabasioglu, M. Celik and L. Pileggi. Prima: Passive reduced-order interconnect macromodeling algorithm. *IEEE Transactions on Computer-Aided Design*, 17(8):645–654, August 1998.

[14] A. Dounavis, R. Achar, and M. S. Nakhla. Passive macromodels for distributed high-speed networks. *IEEE Transactions on Microwave Theory and Techniques*, pages 1686–1696, October 2001.

[15] A. C. Cangellaris, S. Pasha, J. Prince and M. Celik. A new discrete time-domain model for passive model-order reduction and macromodeling of high-speed interconnections. *IEEE Transactions on Components, Packaging, and Manufacturing Technology*, pages 356–364, August 1999.

[16] A. Dounavis, R. Achar, and M. S. Nakhla. On passive time-domain macromodels of distributed transmission-line networks. In *Digest of the IEEE International Microwave Symposium*, volume to appear, June 2002.

[17] T. V. Nguyen. Efficient simulation of lossy and dispersive transmission lines. In *Proc. of the Design Automation Conference*, volume 31, pages 622–627, June 1994.

[18] D. B. Kuznetsov and J. E. Schutt-Ainé. Optimal transient simulation of transmission lines. *IEEE Transactions on Circuits and Systems, I*, 43(2):110–121, February 1996.

[19] R. D. Kimmel. IBM simulator DLL interface: Version 1.0. Circuit design and analysis, IBM Microelectronics Division, October 2001.

[20] J. Morsley, K. Coperich, V. Okhmatovski, A. C. Cangellaris and A. Ruehli. A new broadband transmission line model for accurate simulation of dispersive interconnects. In *Electr. Packaging Technology Conference*, volume 3, pages 345–351, Signapore, December 2000.